View Article Online
View Journal

Chemical
Science

This article can be cited before page numbers have been issued, to do this please use: H. Li, B. Xi, H. Jing, X. Li, H. Jia, M. Fan, W. Zhu, R. Feng, B. Hao, S. Li, B. Yu, Y. Lan and J. Du, *Chem. Sci.*, 2026, DOI: 10.1039/D6SC02310J.

ROYAL SOCIETY
OF CHEMISTRY

rsc.li/chemical-science

View Article Online
DOI: 10.1039/D6SC02310J

ARTICLE

Photo-Induced Terminal Alkyne Insertion into Arene Ring to Synthesize Boron-Doped Polycycles

Received 00th January 20xx,
Accepted 00th January 20xx

DOI: 10.1039/x0xx00000x

Hai-Jun Li,[a] Biying Xi,[a] Hui-Xian Jing,[a] Xin Li,[a] Hongnan Jia,[a] Manman Fan,[a] Weiguo Zhu,[a] Rui Feng,*[b] Baorui Hao,[a] Shi-Jun Li,*[a] Bing Yu,*[a] Yu Lan,[a] and Jingzhen Du*[a]

The classic Büchner reaction involves the insertion of highly reactive carbenoids into benzene rings to form cycloheptatrienes. Achieving a Büchner-type ring expansion using stable terminal alkynes as carbon sources, however, has remained a formidable challenge. Herein, we report that under light irradiation, ethynyl- and BMes$_2$ (Mes = 2,4,6-trimethylphenyl)-substituted heteroarenes undergo an intramolecular Büchner-type ring expansion. This clean reaction generates heteroatom-doped polycyclic compounds through concerted inert aromatic C–C bond cleavage, carbon atom insertion, and hydrogen atom transfer (HAT). To our knowledge, this is the first example of a Büchner-type ring expansion employing a stable terminal alkyne to form a C7 ring, offering a new strategy for constructing boron-containing polycyclic architectures. Theoretical studies reveal that the photochemical transformation is enabled by intramolecular allene- and boron-radical species along with an intramolecular HAT process.

Introduction

Arene compounds are fundamental in organic chemistry and widely utilized in pharmaceuticals, petrochemicals, and materials science.[1,2] Over decades, the functionalization and transformation of arenes via C–H activation[3-5] or dearomatization[6,7] have been well-established. In contrast, the activation of arene ring's C=C bonds for skeletal modification remains challenging under mild conditions, largely due to the inherent aromaticity, low polarity, and competitive C–H functionalization pathways of arenes.[8-17] Nevertheless, the selective cleavage of aromatic C=C bonds offers a promising strategy for the efficient modification of arene rings and their conversion into high-value compounds.[1,18-23]

The Büchner ring expansion represents a classic example of carbon-atom insertion into the inert C=C bond of a benzene ring, typically leading to the formation of a seven-membered ring. Traditional versions of this reaction rely on highly reactive carbene species as the carbon source, which often afford mixtures of cycloheptatriene isomers with low regioselectivity (Figure 1a).[24-26] The introduction of precious-metal catalysts has significantly advanced this field, substantially improving regioselectivity in Büchner-type reactions (Figure 1b).[27-34]

Beyond transition metals, highly reactive low-valent main-group species have also demonstrated the capability to participate in aromatic ring expansion processes.[35-41] For example, in 2002, Kira and co-workers reported that a silylene can undergo Büchner-type ring expansion reactions with benzene and toluene via insertion of the Si atom into aromatic C=C bond under photochemical conditions (Figure 1a).[42] Okazaki and co-workers later observed the [1+2] cycloaddition and ring expansion reactions of silylenes and aromatic compounds under thermal conditions.[43] More recently, Inoue, Rieger and co-workers demonstrated that acyclic iminosilylene compounds can undergo either intramolecular or intermolecular Büchner-type ring expansion by inserting the Si atom into aromatic C=C bonds, with the reaction outcome depending on the substituents on silicon.[26,44] Notably, Goicoechea, Aldridge and co-workers described a rare example of an isolable low-valent aluminium compound [K(2.2.2-crypt)][(NON)Al] (NON = 4,5-bis(2,6-diisopropyl-anilido)-2,7-di-*tert*-butyl-9,9-dimethylxanthene)-involved oxidative activation of the C=C bond in benzene to afford a seven-membered AlC$_6$H$_6$ metallacycle at room temperature (Figure 1a).[45]

In transition-metal-free systems, photochemical strategies have been proven effective for cleaving aromatic C=C bonds and transforming arene skeletons, often by generating highly reactive radical intermediates, particularly with lighter main group elements such as N, C, and B.[46-51] Early work by Sundberg, DeGraff, Chapman and co-workers in the 1970s showed that photolysis of phenyl azide with amines afforded N-insertion products via nitrene intermediates.[9,52,53] More recently, Ruffoni, Leonori and co-workers demonstrated that blue-light irradiation of nitroarenes generates a singlet nitrene capable of Büchner-type expansion to form azepanes.[23] Impressively, Hudnall and co-workers found that photolysis at

---

[a] College of Chemistry, Zhengzhou University, Zhengzhou 450001, China. Emails: lishijunzong@zzu.edu.cn; bingyu@zzu.edu.cn; jingzhendu@zzu.edu.cn
[b] Department of Chemistry, Capital Normal University, Beijing 100048, China. Email: cnufengrui@cnu.edu.cn

† Footnotes relating to the title and/or authors should appear here.

Supplementary Information available: [details of any supplementary information available should be included here]. See DOI: 10.1039/x0xx00000x

View Article Online
DOI: 10.1039/D6SC02310J

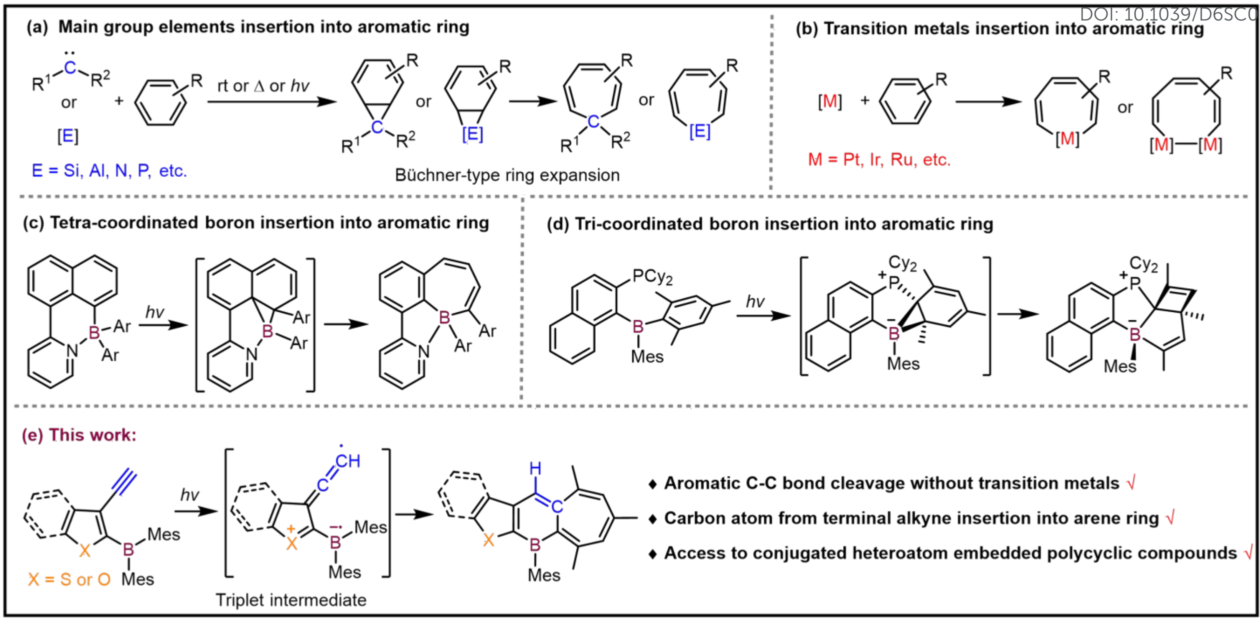

Figure 1. Conceptual overview of previously reported examples of Büchner-type ring expansion reactions (a-d) and summary of this work (e).

380 nm switches a diamidocarbene from singlet to triplet spin state, enabling reversible Büchner-type reactions with arenes.[24] In the related boron chemistry, Wang, Li et al. reported that peri-(2-pyridyl)- and BMes$_2$-substituted naphthalene/acenaphthene derivatives undergo B-atom insertion into the arene ring with mesityl migration, yielding benzoborepins (Figure 1c).[54] Takaya and co-workers later showed that ortho-phosphino-substituted triarylboranes undergo reversible boron insertion upon irradiation, producing borabicyclo[3.2.0]heptadiene derivatives (Figure 1d).[55] Despite these advances in main-group-atom insertion into arenes, especially *via* carbene pathways,[56] the corresponding process employing a stable terminal alkyne as a C1 source remains unknown. While transition metals have been shown to promote the insertion of internal alkynes into arenes to form expanded C7 rings,[57,58] the cleavage of an aromatic C=C bond and insertion of a Csp atom from a terminal alkyne without any metal has not been reported.

The electron-deficient character of boron endows boron-incorporated conjugated molecules with distinct electronic properties,[59] rendering them valuable in organic synthesis[60-62] and optoelectronic materials.[63,64] Boron also plays a key role in photoinduced transformations, enabling the conversion of simple boron-containing frameworks into complex architectures through photoisomerization.[65-70] Moreover, photo-promoted ring opening and boron-insertion reactions offer a direct route to novel boron-doped organic molecules (Figures 1c and 1d), which have potential applications in organic functional materials.[54,55]

Inspired by the above photo-promoted Büchner-type ring expansion reactions, particularly those involving boron-engaged photo-transformation, we designed and synthesized a series of air-stable BMes$_2$-substituted aromatic heterocycles bearing an adjacent ethynyl group to exploit potential synergy between the boron center and the alkyne under UV light irradiation (Figure 1e). We found that the carbon atom of the terminal ethynyl group inserts into a robust C=C bond of a mesityl ring, assisted by the boron atom, without the need for harsh conditions or highly reactive substrates (Figure 1e and 2a). This work establishes a new strategy for arene C=C bond cleavage/insertion and provides access to novel, highly conjugated polycyclic boron compounds fused with various aromatic rings, which are challenging to prepare by conventional methods.

Results and Discussion

Synthesis and Characterization

The 2-dimesitylboryl-3-ethynyl-heteroarene compounds **1a**-**1e** were prepared by modified two-step reactions (See Supporting Information). First, 2-bromo-3-ethynylheteroarene or 3-ethynylheteroarene derivatives with a trimethylsilane protecting group at the terminal carbon atom of the alkynyl group were lithiated, followed by quenching with FBMes$_2$ to afford the dimesitylboryl-substituted intermediates **pre-1a** to **pre-1d** in moderate to high yields (33%-84%). Subsequent deprotection with TBAF to remove the trimethylsilyl group gave the target compounds **1a**-**1d** in high yields (80%-95%). The deuterated compound **1e** was prepared by lithiation of **1b** and followed by quenching with D$_2$O. They were characterized by multi-nuclear NMR spectra (^{1}H, ^{13}C{^{1}H}, ^{11}B{^{1}H} NMR spectra) and HRMS analysis. The crystal structures of **1a**-**1d** were also determined by single-crystal X-ray diffraction analysis (Figures 4a and See Supporting Information Figure S25-S28), and the DFT-optimized structures agree well with the crystallography data.

View Article Online
DOI: 10.1039/D6SC02310J

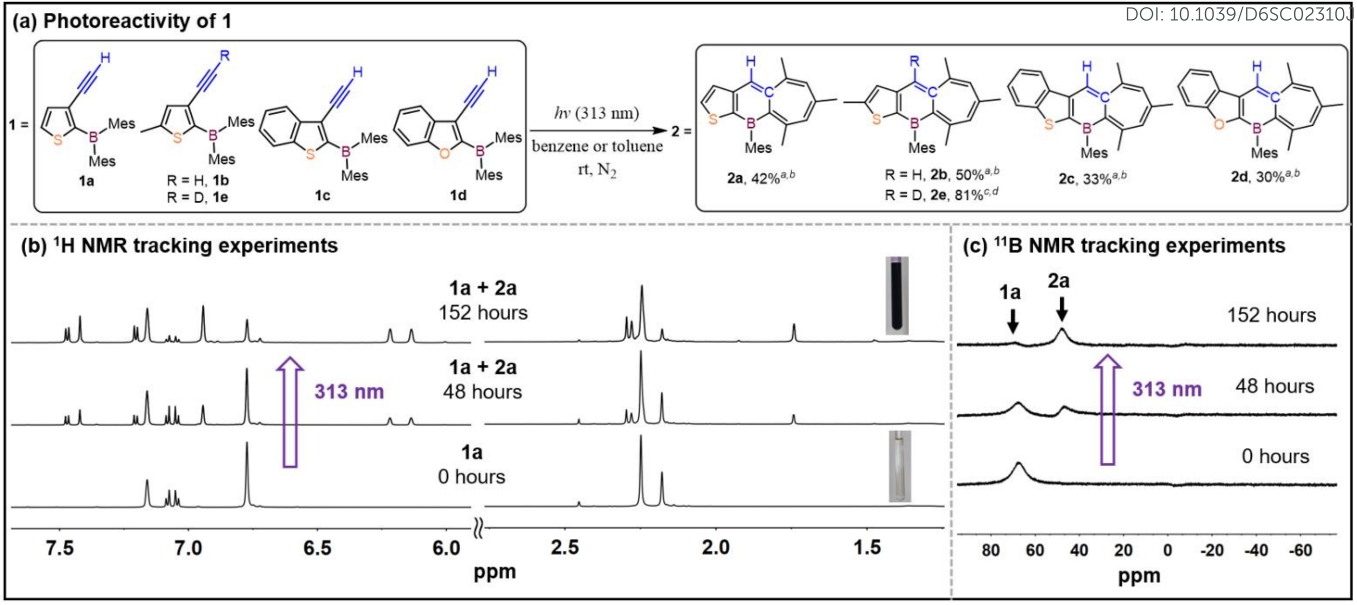

Figure 2. (a) Photo-promoted transformation of **1** to **2**; ^{1}H NMR (b) and ^{11}B NMR (c) tracking experiments show the conversion of **1a** to **2a** in C_6D_6 under 313 nm light irradiation at room temperature. [a]10 days. [b]isolated yields, [c]174 hours. [d]NMR yield.

These compounds all have strong and broad absorption bands at λ_{abs} = 275 to 400 nm (ε = 7200 to 21100 mol^{-1} cm^{-1}), and exhibit weak emission with λ_{em} = 422 to 452 nm, $\Phi_{FL} \approx 0.2\% - 5.6\%$ and with the apparent Stokes shift (6809 cm^{-1}, 5826 cm^{-1}, 5646 cm^{-1}, 5654 cm^{-1} for **1a**-**1d** respectively) owing to a charge transfer from the mesityl group (π, HOMO) to the boron center (p_{π}, LUMO) (See Supporting Information Figures S22, S23, Table S1).

Photochemical Reactivity Studies

Compounds **1a**-**1d** could be isolated by column chromatography on silica gel, and do not decompose after heating to 70 °C (Figure S11). So, they are air- and thermally-stable, but they are all sensitive to UV light irradiation, typically with a notable color change from colorless to dark purple (**2a**, **2b**, **2d**) or green (**2c**). First, we carried out the photochemical reactivity study with 2-dimesitylboryl-3-ethynylthiophene (**1a**) as the starting material. A solution of **1a** (5.0 mg in 0.5 mL toluene-d_8 or benzene-d_6) was irradiated with a UV light source (313 nm, 160 W) at room temperature under N_2 atmosphere. The colorless solution gradually turned into dark purple solution after several hours of irradiation (Figure 2b), and the UV-vis absorption spectrum of **2a** exhibits a new broad band at λ ≈ 550 nm (Figure 4c). Monitoring the photoreaction by ^{1}H and ^{11}B{^{1}H} NMR spectra revealed that this reaction was clean with high regioselectivity without any detectable intermediates and only produced one product **2a** with some starting material **1a** leftover after more than 100 hours of irradiation (Figure 2b and 2c). Transient absorption spectroscopy revealed that the conversion from **1** to **2** takes only around 7 ns, making the detection and capture of the intermediates difficult (Figure S15). EPR and radical trapping experiments were used to investigate the involvement of the radical intermediates in this photo-transformation process (Figures S16, S19-S21). The ^{11}B{^{1}H} NMR spectrum showed two resonance signals at δ = 67.50 and 47.82 ppm, and the former signal belongs to the starting material **1a**, while another upfield shifted resonance signal corresponds to the product **2a** which is similar to other trisubstituted boron-containing compounds featuring B=N[71] or B=C[72,73] bond. After around 150 hours of irradiation, the ^{1}H and ^{11}B{^{1}H} NMR spectra indicated that around 76% of **1a** was consumed and converted into the product **2a** based on the ^{1}H NMR spectra. Importantly, compound **2a** is air-stable and can be purified by silica gel column chromatography. The photoreaction can be performed on a large synthetic scale to prepare **2a** in 42% isolated yield. The ^{1}H NMR spectrum (in THF-d_8) of isolated **2a** was consistent with the spectrum of the product generated in the photoreaction of the NMR tracking experiments, where singlet alkenyl protons were observed at

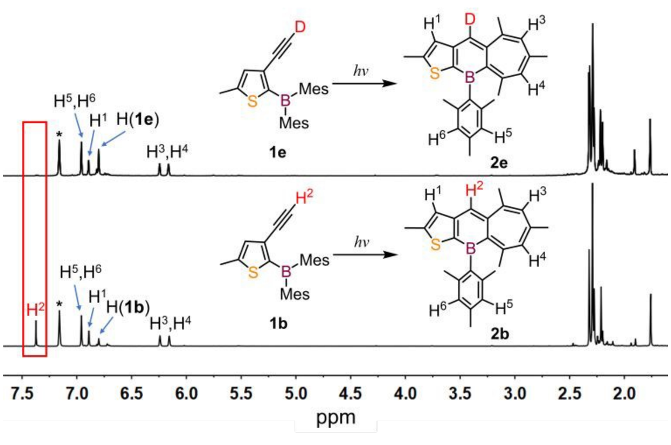

Figure 3. Comparison of the ^{1}H NMR spectra of a mixture of **1b**, **2b** (bottom, 5 mg of **1b** in C_6D_6 irradiated at 313 nm for 48 hours) and a mixture of deuterium-labelling **1e**, **2e** (top, 10 mg of **1e** in C_6D_6 irradiated at 313 nm for 48 hours) with the assignment of the aromatic peaks. The solvent peaks are labelled with *.

View Article Online
DOI: 10.1039/D6SC02310J

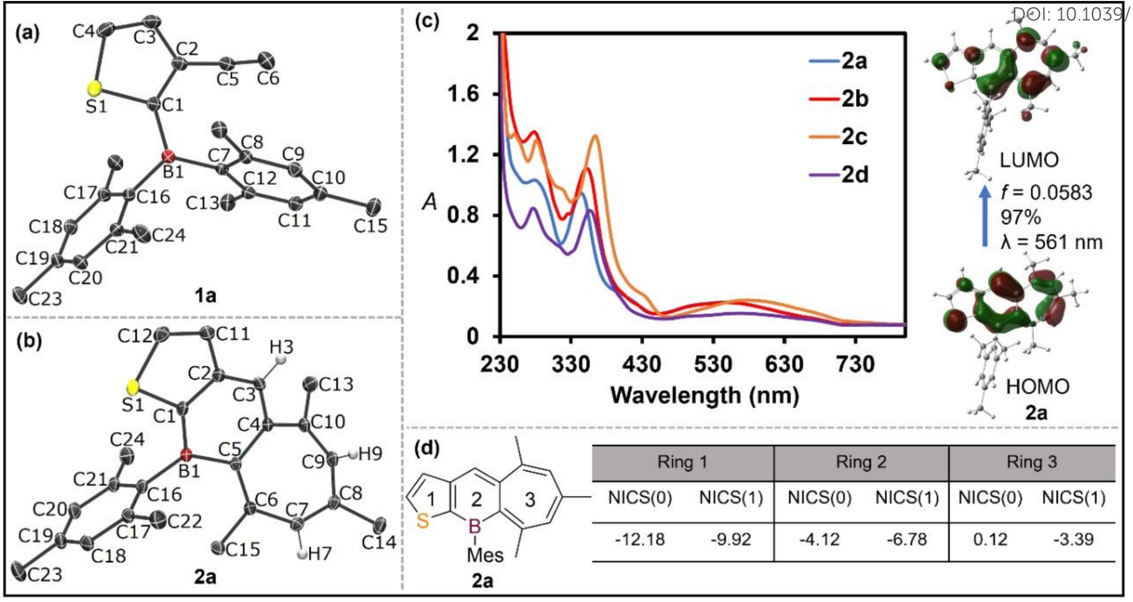

Ring 1		Ring 2		Ring 3	
NICS(0)	NICS(1)	NICS(0)	NICS(1)	NICS(0)	NICS(1)
-12.18	-9.92	-4.12	-6.78	0.12	-3.39

Figure 4. Crystal structures of **1a** (a) and **2a** (b), thermal ellipsoids set at 30% probability, hydrogen atoms are omitted for clarity, selected bond lengths [Å] and angles [°] for **1a**: B1-C1: 1.546 (3), B1-C7: 1.578 (3), B1-C16: 1.581 (3), C1-C2: 1.391(3), C2-C5: 1.404(3), C5-C6: 1.215(3); for **2a**: B1-C1: 1.518(2), B1-C5: 1.5733(18), B1-C16: 1.5808(18), C1-C2: 1.3931(19), C2-C3: 1.4345 (18), C3-C4: 1.3622(19), C4-C5: 1.4877(18), C5-C6: 1.3906(18), C6-C7: 1.4492(18), C7-C8: 1.357(2), C8-C9: 1.435(2), C9-C10: 1.3469(19), C4-C10: 1.4851(17), C10-C13 1.511(2), C11-C12 1.363(2); C1-B1-C5 113.18(11), C5-B1-C16 129.60(12), C1-B1-C16 117.10(11), C2-C1-B1 123.37(11), C1-C2-C3 119.53(12), C2-C3-C4 123.18(12), C3-C4-C5: 121.26(11), C4-C5-B1: 117.22(11). (c) Absorption spectra of **2a**-**2d** in dichloromethane (10^{-4} M) and the calculated HOMO, LUMO diagrams and oscillator strength (*f*) involved in the $S_0 \rightarrow S_1$ vertical excitation (B3LYP/6-31g(d)) for **2a**. (d) Calculated NICS(0), NICS(1) values (ppm) of **2a**.

δ = 7.42, 6.57, 6.47 ppm with only one mesityl aromatic Mes-H signal at δ = 6.82 ppm (See Supporting Information Figure S73). Compound **2a** was fully characterized by NMR spectroscopic analysis, HRMS, and X-ray crystallography (see the Supporting Information and Figure 4b). The control experiments confirmed that the presence of air (Figure S12) or lowering the temperature (Figure S13) is unfavorable for this photo-transformation.

To investigate the steric and electronic influence of the substrate on this unusual photoreaction, compounds that bear different substituents, heteroarenes, or extended π-conjugated heteroarenes (**1b**-**1d**) were prepared and well characterized (Figure 2a). Compounds **1b**-**1d** undergo similar structural photo-transformation as does **1a**. The photochemical reaction rate and the isolation yield (50%) of **1b** are similar to **1a**. However, for **1c** and **1d**, the prolonged irradiation (30 h) was required for these photo-reactions to produce **2c** and **2d** in ~70% yields, as suggested by in-situ ^{1}H NMR spectroscopic studies (See Supporting Information Figures S3 and S4). It is therefore the conversion rate of the compounds with an additional conjugated benzene ring (**1c** and **1d**) is slightly lower than those of **1a** and **1b** (Figures S8, S9). The products **2b**-**2d** were also characterized by NMR spectroscopy and HRMS. The structures of **2b**-**2d** were disclosed by the single-crystal X-ray diffraction analysis and were found to be similar to **2a** (Figure 4b and See Supporting Information Figures S29-S32). Compound **pre-1a** was taken as an example to investigate the photoreactivity of the internal alkyne substrates. The ^{1}H NMR tracking experiments showed that **pre-1a** does not undergo any structural changes upon irradiation with UV light (Figure S10).

In order to investigate the origin of the proton in the central boron-containing six-membered ring (e.g., H3 in Figure 4b), we carried out the following deuterium labelling reactions. The deuterium labelled compound **1e** was prepared and irradiated under the same conditions as **1a-1d**, which underwent a similar photo-transformation process based on the NMR spectroscopic analysis (Figure 3). Compared with the ^{1}H NMR spectrum of undeuterated **2b**, the typical singlet peak at δ = 7.28 ppm is diagnosed as the proton atom in the boron-containing six-membered ring, which is absent in the ^{1}H NMR of **2e** (Figure 3, top one). In addition, the ^{2}H NMR spectrum of **2e** also detected the D resonance signal at 7.37 ppm (See Supporting Information Figure S98) with a similar chemical shift as in the ^{1}H NMR spectra of **2b** (Figure 3, bottom one). Thus, the deuterium labelling experiments unambiguously confirmed that the H-atom transferred to the Csp^2 atom of the boron-containing six-membered ring originates from the Csp-H of the alkyne group, which is in line with theoretical findings on the mechanism (*vide infra*). These results also highlight the synergistic effect of boron and the terminal alkyne group plays a key role in these unprecedented photo-promoted Büchner-type ring expansion reactions.

Solid-State Structures

The molecular structures of **2a**-**2d** are shown in Figure 4b and the Supporting Information Figures S29-S32, which confirm the presence of a boron-embedded polycyclic framework. Given the structural similarity among **2a**-**2d**, the discussion is focused on the solid-state structure of **2a**, where the fused five-membered ring is derived from the original thiophene five-membered ring. One of the mesityl groups on

View Article Online
DOI: 10.1039/D6SC02310J

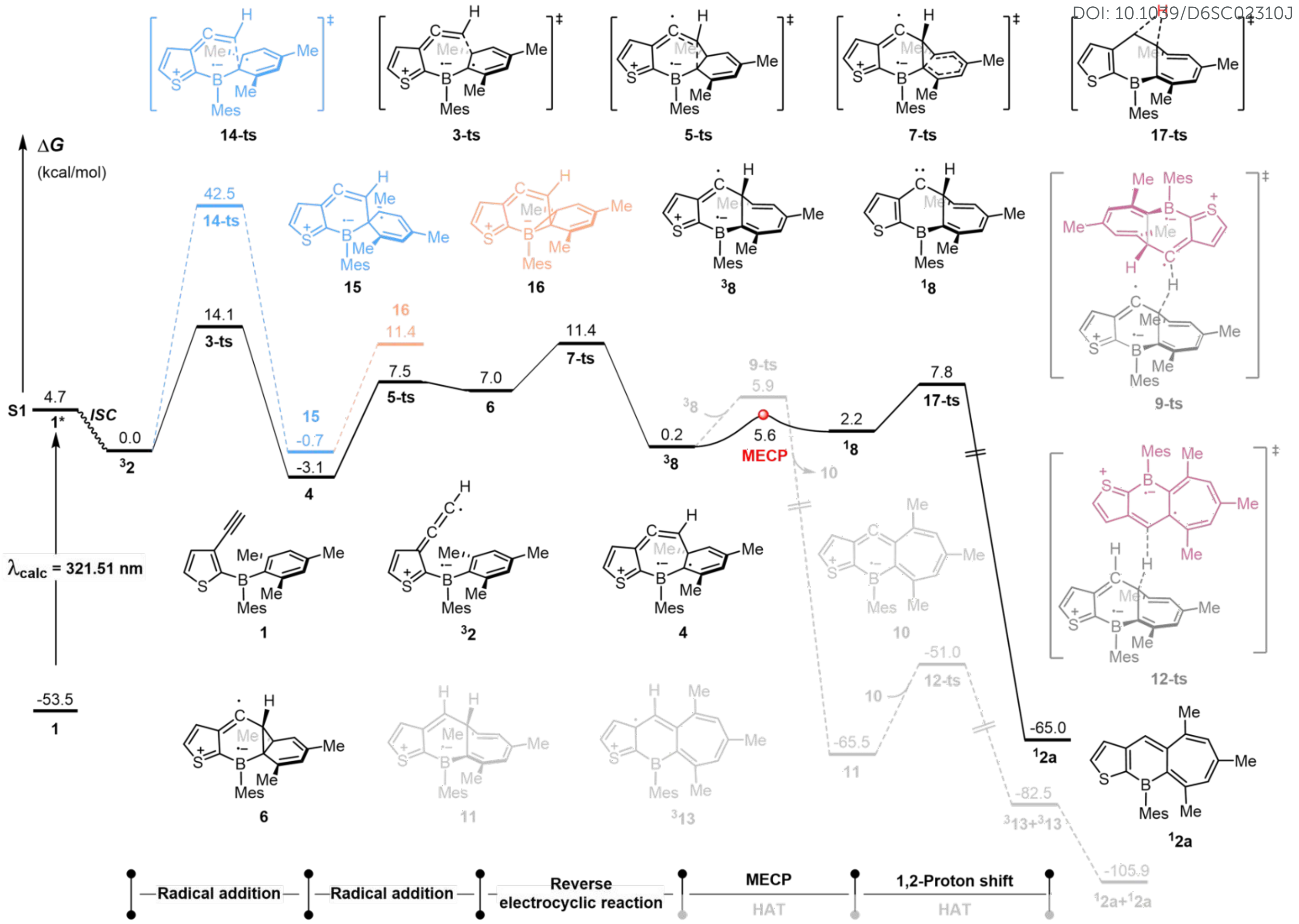

Figure 5 A plausible reaction mechanism and the free energy profile for the light-promoted expansion ring process.

the boron center of the original **1a** was inserted by the terminal Csp atom of the alkynyl group, undergoing Büchner-type ring expansion to form a new seven-membered ring in **2a**. The C≡C bond of **1a** was transformed into a C=C bond in **2a**, which is part of the boron-doped six-membered ring. The newly formed seven-membered ring unit is similar to cycloheptatriene, featuring alternating C=C (~1.32 Å) and C–C bonds (~1.53 Å), which is consistent with the chemical shift of olefinic protons (δ = 6.19 to 6.14 ppm) on the seven-membered ring. However, the difference between **2a** and cycloheptatriene is that seven carbon atoms of the former are all sp^2 hybridized, while in the latter, six C atoms are sp^2 hybridized and one C atom is sp^3 hybridized. The B(1)–C(1) bond length is 1.518(2) Å, which is between the B–C single bond length (B1–C16 = 1.5808(18) Å of **2a**) and reported B=C double bond distances (~1.37-1.44 Å),[74,75] thus suggesting partially double-bond character for the former. In the molecule of **2a**, the C3–C4 bond and all of the seven C–C bonds in the heptagonal ring also have partially double bond character by analyzing the bond lengths (Figure 4b). Thus, the structural data suggest that the polycyclic compounds **2a**-**2d** represent a class of highly conjugated molecules consistent with the intense absorptions in their electronic absorption spectra (Figure 4c). Compounds **2a**-**2d** have very similar absorption bands and a broad band at around 550 nm that is responsible for the dark purple or green color (Figure 4c). TD-DFT theoretical analysis (B3LYP/6-31g(d)) suggests that these absorption bands of **2a**-**2d** originate from charge transfer (CT) transitions involving mainly the HOMOs to LUMOs (Figure 4c and See Supporting Information Table S19-S26) of the conjugated central boron-containing six-membered ring and the newly formed seven-membered ring with highly delocalized π-electronic character.

Density Functional Theory Calculations and Mechanistic Studies

To gain insight into the electronic structure of **2a**-**2d**, density functional theory (DFT) calculations were performed at the B3LYP/6-31g(d) level of theory. The nucleus-independent chemical shift (NICS) values of **2a**-**2d** were calculated to illustrate the aromaticity of these novel polycyclic compounds, and the NICS values are listed in the Supporting Information Tables S27-S30. Both of the NICS(0) and NICS(1) values of the central BC5 six-membered rings are negative (NICS(0) = -4.12, -4.47, -4.57, -5.32 ppm and NICS(1) = -6.78, -6.95, -7.73, -8.09 ppm for **2a**-**2d** respectively), indicating π-aromatic character of the central BC5 six-membered rings in **2a**-**2d**. However, the aromaticity of the central BC5 six-membered rings in **2a**-**2d** is weaker compared with that of the SC4 ring in **2a** with more

View Article Online
DOI: 10.1039/D6SC02310J

negative NICS(0) (-12.18 ppm) and NICS(1) (-9.92 ppm) values, or the phenyl ring in **2c** (NICS(0) = -9.86 ppm and NICS(1) = -11.12 ppm). The C7 seven-membered rings in **2a**-**2d** also show weak aromaticity based on the NICS values (NICS(1) = -3.39, -3.04, -3.24, -3.97 ppm for **2a**-**2d**, respectively).

To gain a deeper understanding of the mechanism in these unprecedented photo-promoted Büchner-type ring expansion reactions, theoretical calculations by using the density functional theory methods have been employed at the B3LYP-D3/Def2-TZVP/SMD(toluene)//B3LYP/6-31G(d,p)/SMD(toluene) level (Figure 5). First, the ground state reactant **1a** absorbs the UV light to generate the excited singlet state with the absorption wavelength of 321.51 nm. After the thermal relaxation and internal conversion, the S1 state of **1** has been located with the free energy of 4.7 kcal/mol, where the free energy of the triplet state species ^{3}**2** is set to relative zero. Subsequently, the excited triplet species ^{3}**2** is formed via intersystem crossing. The two corresponding singly occupied molecular orbitals located on the alkynyl group and boranyl moiety were obtained by DFT calculations for the resulting excited triplet state. This indicates an effective electron transfer from the alkynyl group to the boron atom in the excitation process. Then, the terminal allenyl radical could undergo a radical addition to the phenyl moiety. Considering the possible sites, two pathways will be discussed in the following. In the first pathway, the radical addition to the carbon atom bonded to the methyl group would be quite easily via the transition state **3-ts** with a free energy barrier of only 14.1 kcal/mol, while the radical addition to the carbon atom bonded to the boron center via **14-ts** would be kinetically unfavorable with a very high energy barrier of 42.5 kcal/mol, which is not discussed in further. After the addition, the seven-membered ring intermediate **4** with the allenyl group forms with an exergonicity of 3.1 kcal/mol. Subsequently, the radical undergoes another intramolecular radical addition toc the allenyl moiety, affording the fused ring intermediate **6** via the three-membered ring transition state **5-ts** with a free energy barrier of 10.6 kcal/mol. It should be noted that the fused ring intermediate could open the ring to generate expanded ring intermediate ^{3}**8** via the reverse electrocyclic transition state **7-ts** with a small free energy barrier of 4.4 kcal/mol, accompanied by the release of ring strain. At last, the triplet alkenyl radical could form the final product **2a** with a formal 1,2-hydrogen atom transfer process (HAT). The stepwise intermolecular HAT process proceeds via transition states **9-ts** and **12-ts**, with free energy barriers of 5.7 and 14.5 kcal/mol, respectively. Notably, a minimum energy crossing point (MECP) between the triplet and singlet states of intermediate **8** has also been located, with an energy barrier of 5.4 kcal/mol. Subsequently, a 1,2-proton shift occurs via transition state **17-ts** with a free energy barrier of 5.6 kcal/mol. Considering the concentration of triplet ^{3}**8**, the intramolecular proton shift after MECP would be a favorable pathway with less entropy loss, which is also consistent with the deuterium-labelling experimental results (Figure S14). Furthermore, the trace water, benzene, toluene, and terminal alkyne have also been considered in the 1,2-HAT process, which are unfavorable for these reactions (see the Supporting Information for full details).

Conclusions

To conclude, photolyzing a series of air-stable ethynyl and boron functional groups substituted heteroarenes **1a**-**1d** has enabled us to discover an unprecedented Büchner-type ring expansion reaction to produce boron-doped polycyclic compounds **2a**-**2d**. It should be emphasized that these reactions are the first examples of Büchner-type ring expansion reactions using a stable terminal alkyne group as the carbon atom transfer source to form C7-ring in any synthetic system, developing a new synthetic strategy to boron-containing polycyclic compounds. DFT study on the electronic structures of **2a**-**2d** revealed the π-electron delocalization through the newly formed central boron-containing six-membered ring and seven-membered ring, and the central boron-containing six-membered ring exhibits substantial aromaticity, reflected by calculated NICS values, which is in line with their electronic absorption spectra. Theoretical studies on reaction mechanism revealed that the formation of biradical species, intramolecular HAT process, and the synergistic effect of boron and terminal alkyne group are of importance for this complex photo-transformation involving many chemical bond cleavages and formations. This work not only develops a new strategy to modify the arene skeleton under mild reaction conditions, but also provides a promising way for the construction and functional applications of novel conjugated polycyclic aromatic boron-containing compounds.

Author contributions

H.J.L. conceived the original idea and wrote the manuscript. H.J.L., B.Y. and J.D. supervised the work, analyzed all the data, and proofread the manuscript. B.X., X.L., M.F. and H.J.L synthesized and characterized all the compounds. H.X.J., S.J.L. and Y.L. conducted the computational studies. H.J., R.F. and B.H. analyzed the crystallographic characterization data. R.F. analyzed the EPR spectra. W.Z. and H.J.L. conducted and analyzed the 2D NMR data.

Conflicts of interest

There are no conflicts to declare.

Data availability

Synthetic methods, characterization data, and computational details can be found in the supporting information; CCDC 2456755-2456761, 2483356 contain the supplementary crystallographic data for this paper. These data can be obtained free of charge from The Cambridge Crystallographic Data Centre.

View Article Online
DOI: 10.1039/D6SC02310J

Acknowledgements

We gratefully acknowledge funding and support from the National Natural Science Foundation of China (Nos. 22101007, 22471242, 22509189), the Natural Science Foundation of Henan Province (No. 242300421344), and Zhengzhou University. The authors thank Prof. Xiangkun Jia for assistance with the transient absorption spectroscopy testing and analysis.

Notes and references

1 W. C. Wertjes, E. H. Southgate and D. Sarlah, *Chem. Soc. Rev.*, 2018, **47**, 7996–8017.
2 H. Yorimitsu, *Acc. Chem. Res.*, 2025, **58**, 1323–1334.
3 T. Gensch, M. N. Hopkinson, F. Glorius and J. Wencel-Delord, *Chem. Soc. Rev.*, 2016, **45**, 2900–2936.
4 J. A. Labinger and J. E. Bercaw, *Nature,* 2002, **417**, 507–514.
5 C.-X. Liu, S.-Y. Yin, F. Zhao, H. Yang, Z. Feng, Q. Gu and S.-L. You, *Chem. Rev.*, 2023, **123**, 10079–10134.
6 Y.-Z. Cheng, Z. Feng, X. Zhang and S.-L. You, *Chem. Soc. Rev.*, 2022, **51**, 2145–2170.
7 Y. Wang, W.-Y. Zhang, Z.-L. Yu, C. Zheng and S.-L. You, *Nat. Synth.*, 2022, **1**, 401–406.
8 X. Qiu, Y. Sang, H. Wu, X.-S. Xue, Z. Yan, Y. Wang, Z. Cheng, X. Wang, H. Tan, S. Song, G. Zhang, X. Zhang, K. N. Houk and N. Jiao, *Nature*, 2021, **597**, 64–71.
9 O. L. Chapman and J.-P. L. Roux, *J. Am. Chem. Soc.*, 1978, **100**, 282–285.
10 Y. Tian, M. Jakoobi, R. Boulatov and A. G. Sergeev, *Chem. Sci.*, 2021, **12**, 3568–3579.
11 J. W. Parr and M. R. Crimmin, *Chem. Sci*., 2023, **14**, 11012–11021.
12 H. Zhu, S. Fujimori, A. Kostenko and S. Inoue, *Chem. Eur. J.*, 2023, **29**, e202301973.
13 J. Jian, X. Wu, M. Chen and M. Zhou, *J. Am. Chem. Soc.*, 2020, **142**, 10079–10086.
14 X. Wen, X. Wu and J. Li, *Org. Lett*., 2018, **20**, 1505–1508.
15 N. Komine, J. A. Flores, K. Pal, K. G. Caulton and D. J. Mindiola, *Organometalllics*, 2013, **32**, 3185–3191.
16 X. Kang, G. Luo, L. Luo, S. Hu, Y. Luo and Z. Hou, *J. Am. Chem. Soc.*, 2016, **138**, 11550–11559.
17 W. Liu, P. Wu, Y. Liang, J. Wei, G. Luo and W.-X. Zhang, *J. Am. Chem. Soc.*, 2025, **147**, 1300–1306.
18 S. Tashiro, M. Yamada and M. Shionoya, *Angew. Chem. Int. Ed*., 2015, **54**, 5351–5354.
19 D.-H. Liu and J. Ma, *Angew. Chem. Int. Ed*., 2024, **63**, e202402819.
20 R. Remy and C. G. Bochet, *Chem. Rev.*, 2016, **116**, 9816–9849.
21 U. Streit and C. G. Bochet, *Beilstein J. Org. Chem*., 2011, **7**, 525–542.
22 Z. Siddiqi, W. C. Wertjes and D. Sarlah, *J. Am. Chem. Soc.*, 2020, **142**, 10125–10131.
23 R. Mykura, R. Sánchez-Bento, E. Matador, V. Duong, A. Varela, L. Angelini, R. J. Carbajo, J. Llaveria, A. Ruffoni and D. Leonori, *Nat. Chem.*, 2024, **16**, 771–779.
24 T. A. Perera, E. W. Reinheimer and T. W. Hudnall, *J. Am. Chem. Soc.*, 2017, **139**, 14807–14814.
25 S. E. Reisman, R. R. Nani and S. Levin, *Synlett,* 2011, **17**, 2437–2442.
26 H. Zhu, A. Kostenko, D. Franz, F. Hanusch and S. Inoue, *J. Am. Chem. Soc.*, 2023, **145**, 1011–1021.
27 A. Sattler and G. Parkin, *Nature*, 2010, **463**, 523–526.
28 S. Hu, T. Shima and Z. Hou, *Nature*, 2014, **512**, 413–415.
29 A. P. Y. Chan and A. G. Sergeen, *Coord. Chem. Rev*., 2020, **413**, 213213.
30 M. Jakoobi, Y. Tian, R. Boulatov and A. G. Sergeev, *J. Am. Chem. Soc.*, 2019, **141**, 6048–6053.
31 M. Jakoobi and A. G. Sergeev, *Chem. Asian. J.*, 2019, **14**, 2181–2192.
32 J. Browning, M. Green, A. Laguna, L. E. Smart, J. L. Spencer and F. G. A. Stone, *J. Chem. Soc. Chem. Commun*., 1975, 723–724.
33 M. Jakoobi, N. Halcovitch, G. F. S. Whitehead and A. G. Sergeev, *Angew. Chem. Int. Ed*., 2017, **56**, 3266–3269.
34 T. Li, J.-J. He, K.-Y. Fan, L.-W. Ye, B. Zhou and X.-Q. Zhu, *Org. Chem. Front*., 2025, **12**, 1966–1972.
35 H. Li, N. Li, J. Wu, T. Yu, R. Zhang, L.-P. Xu and H. Wei, *J. Am. Chem. Soc.*, 2023, **145**, 17570–17576.
36 R. H. Kern, M. Schneider, K. Eichele, H. Schubert, H. F. Bettinger and L. Wesemann, *Angew. Chem. Int. Ed*., 2023, **62**, e202301593.
37 C. Xu, Z. Ye, L. Xiang, S. Yang, Q. Peng, X. Leng and Y. Chen, *Angew. Chem. Int. Ed*., 2021, **60**, 3189–3195.
38 L. Zhu, J. Zhang and C. Cui, *Inorg. Chem*., 2019, **58**, 12007–12010.
39 L. L. Liu, J. Zhou, L. L. Cao, R. Andrews, R. L. Falconer, C. A. Russell and D. W. Stephan, *J. Am. Chem. Soc.*, 2018, **140**, 147–150.
40 L. L. Liu, L. L. Cao, J. Zhou and D. W. Stephan, *Angew. Chem. Int. Ed*., 2019, **58**, 273–277.
41 X. Zhang and L. L. Liu, *Angew. Chem. Int. Ed*., 2022, **61**, e202116658.
42 M. Kira, S. Ishida, T. Iwamoto and C. Kabuto, *J. Am. Chem. Soc.*, 2002, **124**, 3830–3831.
43 H. Suzuki, N. Tokitoh and R. Okazaki, *J. Am. Chem. Soc.*, 1994, **116**, 11572–11573.
44 D. Wendel, A. Porzelt, F. A. D. Herz, D. Sarkar, C. Jandl, S. Inoue and B. Rieger, *J. Am. Chem. Soc.*, 2017, **139**, 8134–8137.
45 J. Hicks, P. Vasko, J. M. Goicoechea and S. Aldridge, *J. Am. Chem. Soc.*, 2019, **141**, 11000–11003.
46 N. P. Gritsan, A. D. Gudmundsdóttir, D. Tigelaar, Z. Zhu, W. L. Karney, C. W. Hadad and M. S. Platz, *J. Am. Chem. Soc*., 2001, **123**, 1951–1962.
47 Y.-A. Xu, S.-H. Xiang, J.-T. Che, Y.-B. Wang and B. Tan, *Chin. J. Chem*., 2024, **42**, 2656–2667.
48 C. Wentrup, *Angew. Chem. Int. Ed*., 2018, **57**, 11508–11521.
49 S. K. Mellerup and S. Wang, *Sci. China Mater*., 2018, **61**, 1249–1256.
50 M. Kira, S. Ishida, T. Iwamoto, A. Meijere, M. Fujitsuka and O. Ito, *Angew. Chem. Int. Ed*., 2004, **43**, 4510–4512.
51 N. P. Gritsan and M. S. Platz, *Chem. Rev*., 2006, **106**, 3844–3867.
52 R. J. Sundberg, B. P. Das and R. H. Smith Jr, *J. Am. Chem. Soc.,* 1969, **91**, 658–668.
53 B. A. DeGraff, D. W. Gillespie and R. J. Sundberg, *J. Am. Chem. Soc*., 1974, **96**, 7491–7496.
54 S. Wang, K. Yuan, M.-F. Hu, X. Wang, T. Peng, N. Wang and Q.-S. Li, *Angew. Chem. Int. Ed*., 2018, **57**, 1073–1077.
55 K. Kuroki, T. Ito and J. Takaya, *Angew. Chem. Int. Ed*., 2023, e202312980.
56 F. Xu and J. Zhu, *Chem. Eur. J*., 2023, **29**, e202203216.
57 T. Matsuda, T. Goya, L. Liu, Y. Sakurai, S. Watanuki, N. Ishida and M. Murakami, *Angew. Chem. Int. Ed*., 2013, **52**, 6492–6495.
58 Y.-X. Zheng, L.-G. Liu, T.-Q. Hu, X. Li, Z. Xu, X. Hong, X. Lu, B. Zhou and L.-W. Ye, *Nat. Commun*., 2024, **15**, 9227.
59 S. K. Mellerup and S. Wang, *Chem. Soc. Rev*., 2019, **48**, 3537–3549.
60 Z. Liu, Z.-J. Shi, L. Liu, M. Zhang, M.-C. Zhang, H.-Y. Guo and X.-C. Wang, *J. Am. Chem. Soc*., 2023, **145**, 11789–11797.
61 M. Tian, J. Zhang, L. Guo and C. Cui, *Chem. Sci*., 2021, **12**, 14635–14640.
62 E. C. Neeve, S. J. Geier, I. A. I. Mkhalid, S. A. Westcott and T. B. Marder, *Chem. Rev*., 2016, **116**, 9091–9161.
63 M. Hirai, N. Tanaka, M. Sakai and S. Yamaguchi, *Chem. Rev*., 2019, **119**, 8291–8331.
64 H.-J. Li, S. K. Mellerup, X. Wang and S. Wang, *Org. Lett*., 2019, **21**, 2838–2842.
65 S. K. Mellerup, C. Li, J. Radtke, X. Wang, Q.-S. Li and S. Wang, *Angew. Chem. Int. Ed*., 2018, **57**, 9634–9639.
66 N. Ando, A. Fukazawa, T. Kushida, Y. Shiota, S. Itoyama, K. Yoshizawa, Y. Matsui, Y. Kuramoto, H. Ikeda and S. Yamaguchi, *Angew. Chem. Int. Ed*., 2017, **56**, 12210–12214.
67 A. Iida, S. Saito, T. Sasamori and S. Yamaguchi, *Angew. Chem. Int. Ed*., 2013, **52**, 3760–3764.
68 H. Wang, J. Zhang and Z. Xie, *Angew. Chem. Int. Ed*., 2017, **56**, 9198–9201.
69 B. Su, Y. Li, R. Ganguly and R. Kinjo, *Angew. Chem. Int. Ed*., 2017, **56**, 14572–14576.
70 T. Ito, N. Iwasawa and J. Takaya, *Angew. Chem. Int. Ed*., 2020, **59**, 11913–11917.
71 S. K. Mellerup, C. Li, T. Peng and S. Wang, *Angew. Chem. Int. Ed*., 2017, **56**, 6093–6097.
72 M. M. Olmstead, P. P. Power, K. J. Weese and R. J. Doedens, *J. Am. Chem. Soc*., 1987, **109**, 2541–2542.

View Article Online
DOI: 10.1039/D6SC02310J

73 B. G. Ramsey and L. M. Isabelle, *J. Org. Chem.*, 1981, **46**, 179–182.
74 R. Hunold, M. Pilz, J. Allwohn, M. Stadler, W. Massa, P. R. Schleyer and A. Berndt, *Angew. Chem. Int. Ed. Engl.*, 1989, **28**, 781–784.
75 R. Boese, P. Paetzold and A. Tapper, *Chem. Ber.*, 1987, **120**, 1069–1071.

View Article Online
DOI: 10.1039/D6SC02310J

Data Availability Statement

Synthetic methods, characterization data, and computational details can be found in the supporting information; CCDC 2456755-2456761, 2483356 contain the supplementary crystallographic data for this paper. These data can be obtained free of charge from The Cambridge Crystallographic Data Centre.

Jingzhen Du

Jingzhen Du (on behalf of all authors)